Acoustic Tomography Based on Wave Equation

Reza Parhizkar

School of Computer and Communication Sciences
Audiovisual Communications Laboratory (LCAV)

Advisor
Dr. Ivana Jovanović
Ali Hormati
Prof. Martin Vetterli

January 19, 2008

Abstract

In the forward problem of acoustic tomography, one needs to be able to implement the wave equation numerically and find the values at each receiver point. In this research the possible solutions are studied and their properties are discussed and one proposed algorithm is selected as the satisfactory result in the sense of less numerical dispersion. Stability conditions for these algorithms are also investigated.

I. Introduction

The wave equation is one of the most used partial differential equations. Its various applications include acoustic tomography for sound propagation models, seismology and oceanography. Since the modeling of wave equation analytically is not possible so many efforts has been devoted during the last 30 years to find numerical implementations for the wave equation to mimic the exact result as much as possible. We are interested in the fine grid size case of its implementation which is used for acoustic tomography of breast cancer. Since this is a medical diagnostic setup the accuracy is of most importance, and results must be reliable. Previous works by Jovanović [1] has been done to solve the problem using ray theory and through this project it is tried incorporate the wave equation and ray-theory and in many ways improve the results:

- Use the easy reconstruction of the ray-theory and improve the results by doing the forward problem with wave equation to recognize false sensor readings.
- Use the reconstruction of the ray-theory as an initial approximation for an iterative algorithm to reconstruct the sound speed.
- Use the wave equation by itself to do the inverse reconstruction.

for all of these applications, there is a need to numerically implement the forward problem. In the following some methods are investigated to do this accurately. the outline is as follows; first the problem is introduced, then the Leap-Frog 2 (LF2) scheme is studied in more details and absorbing boundary conditions are derived and after introducing a better method the feasibility of usage of implicit methods is shown. Finally some simulation results are presented.

II. Problem Definition and Implementation

The goal in the first phase of the project has been to model the forward problem in wave-based tomography. Namely, assuming that the inside object is available and then try to find the wave values propagated from a source in the receivers. To do this one needs to incorporate the wave equation

$$\nabla^2 u(\mathbf{r},t) - \frac{1}{c^2(\mathbf{r})}\frac{\partial^2 u(\mathbf{r},t)}{\partial t^2} = q(\mathbf{r},t), \tag{1}$$

where $u(\mathbf{r},t)$ is the sound pressure measured at location $\mathbf{r}$ and time t, $q(\mathbf{r},t)$ is the source term and $c(\mathbf{r})$ is the sound speed at each position $\mathbf{r}$. For this problem, assuming that the changes along third dimension of the object are negligible, we are going to restrict ourself to $\mathbf{r} \in \mathbb{R}^2$ in space. For the forward problem to be solved analytically, one needs to find a close solution for the above wave equation which is not possible for the inhomogeneous medium inside.

A. Numerical Implementation

To be able to find the results of wave propagation one can simulate it numerically knowing the characteristics of the in-the-middle object. For this purpose the region of interest in space is divided into (in our case) rectangular cells in each of which the value for sound speed is known and also the time axis is also discretized to equally distant samples.

Thus doing the following second order central finite difference approximation

$$\begin{aligned} \frac{\partial^2 u(\mathbf{r},t)}{\partial t^2} &= \frac{u(\mathbf{r},t+\Delta t) - 2u(\mathbf{r},t) + u(\mathbf{r},t-\Delta t)}{\Delta t^2} \\ \Big(\frac{\partial^2 u(\mathbf{r})}{\partial t^2}\Big)^n &= \frac{u^{n+1}(\mathbf{r}) - 2u^n(\mathbf{r}) + u^{n-1}(\mathbf{r})}{\Delta t^2} \end{aligned} \tag{2}$$

where

$$u^n(\mathbf{r}) = u(\mathbf{r}, n\Delta t), \quad n = 0, 1, 2, \cdots$$

and putting it in (1), leads to

$$u^{n+1}(\mathbf{r}) = \Delta t^2 c^2(\mathbf{r})[\nabla^2 u(\mathbf{r}) - q(\mathbf{r})^n] + 2u^n(\mathbf{r}) - u^{n-1}(\mathbf{r}) \tag{3}$$

In our problem the source is assumed to be a point source and thus the response in space is a dirac and in time a desired signal to be sent towards the receivers

$$s(\mathbf{r}, t) = s(t)\delta(\mathbf{r} - \mathbf{r}_{src}) \tag{4}$$

So assuming that the source is changing very smoothly in space and time as in [2] we can implement it as a hard source and get rid of the $q(\mathbf{r})$ in (3) and impose the source values to $u(\mathbf{r}_{src}, t)$ during the simulations.

Now the only remaining part to make the approximation is to find a good replacement for $\nabla^2 u(\mathbf{r})$. In this regard many efforts has been done and several schemes introduced to implement the second derivatives in space. one can name Leap-Frog 2 (LF2), Leap-Frog 4 (LF4), Crank-Nicolson (CN), Optimal Nearly Analytic Discrete Method (ONADM), implicit methods and Alternative Direct Implicit (ADI) method. In the sequel the LF2 and ONADM are discussed in details and implicit methods are introduced and the reason of why they cannot be used in our problem is discussed.

B. Leap-Frog 2 Scheme

One method to replace the laplacian operator in (3) to use the second order central difference with respect to x and y.

$$\begin{aligned}\nabla^2 u^n(\mathbf{r})\big|_{\mathbf{r}=(i\Delta x, j\Delta y)} = &\frac{u^n_{i+1,j} - 2u^n_{i,j} + u^n_{i-1,j}}{\Delta x^2} \\ &+ \frac{u^n_{i,j+1} - 2u^n_{i,j} + u^n_{i,j-1}}{\Delta y^2}.\end{aligned} \tag{5}$$

Putting the above expression in (3), one gets the updating formula for the wave equation to be

$$u^{n+1}_{i,j} = \Delta t^2 c^2_{i,j}[\frac{u^n_{i+1,j} - 2u^n_{i,j} + u^n_{i-1,j}}{\Delta x^2} + \frac{u^n_{i,j+1} - 2u^n_{i,j} + u^n_{i,j-1}}{\Delta y^2}] + 2u^n_{i,j} - u^{n-1}_{i,j}. \tag{6}$$

Advantage of this method is that it is simple and assuming that $\Delta x = \Delta y$, which is a natural assumption in simulations, one can rewrite it in a matrix form. Assuming that $\mathbf{U}^n$ contains all values of $u_{i,j}$ at time $n\Delta t$, and $\mathbf{C}$ contains the sound speed values in each grid point, (6) can be written as

$$\mathbf{U}^{n+1} = 2\mathbf{U}^n - \mathbf{U}^{n-1} + \frac{\Delta t^2}{\Delta x^2}\mathbf{C}^{②} \odot (\mathbf{U}^n * \mathbf{h}), \tag{7}$$

where $\mathbf{C}^{②}$ is the component-wise square and $\odot$ is component-wise multiplication and

$$\mathbf{h} = \begin{bmatrix} 0 & 1 & 0 \\ 1 & -4 & 1 \\ 0 & 1 & 0 \end{bmatrix}. \tag{8}$$

Thus as the above formula implies most complexity of the algorithm is due to filtering $\mathbf{U}$.

1) CourantFriedrichsLewy Stability Condition: For the moment suppose the wave equation is studied in homogeneous medium. According to [3], we will derive the stability condition for LF2 scheme.

If one rearranges (6) in the following way

$$u^{n+1}_{i,j} = 2(1 - 2\lambda^2)u^n_{i,j} + \lambda^2(u^n i + 1, j + u^n_{i-1,j} + u^n i, j + 1 + u^n_{i,j-1}) - u^{n-1}_{i,j} \tag{9}$$

can define

$$\lambda = \frac{c\Delta t}{\Delta x} \tag{10}$$

Equation (9), allows one to find the value of u at point $P = (x_0, y_0, t_0)$ uniquely as a function of the initial values of the function at planes $t = 0$ and $t = 1$.

The grid points that influence the value of u at P lie inside a pyramid with base on $t = 1$ which is of the form of a rhombus. They call this rhombus as the *domain of dependence* of the difference scheme. Obviously the domain of dependence of the wave equation by itself is a circle in the same plane. Courant, Friedriche and Lewy in [4] showed that for the difference scheme in (9) to be convergent for all smooth initial data the condition is that the rhombus of dependence of the difference scheme must contain the circle of dependence of the differential equation in its interior. With this condition and assuming that $P = (0, 0, n\Delta t)$, the domain of dependence as illustrated in Fig.1 is the circle $x^2 + y^2 \leq (cn\Delta t)^2$. Also as shown in the same

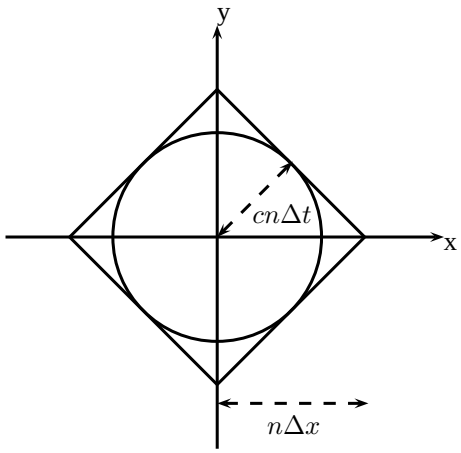

Fig. 1 – Domain of dependence of a point $P = (0, 0, n\Delta t)$ for wave equation (circle) and the difference scheme (rhombus) for LF2. the C.F.L. condition implies that the domain of dependence of the numerical scheme contain the domain of dependence of the wave equation.

figure, the rhombus of dependence of the difference scheme has diameters equal to $2n\Delta x$. So the C.F.L. condition is satisfied provided that

$$\lambda = \frac{c\Delta t}{\Delta x} \leq \frac{1}{\sqrt{2}}. \tag{11}$$

Actually it can be shown that the C.F.L. condition for a LF2 scheme of s-dimensional wave equation is

$$\lambda \leq \frac{1}{\sqrt{2}}. \tag{12}$$

It can be deduced form the above discussions that if the medium is not homogeneous the C.F.L. condition will be

$$\frac{c_{\max}\Delta t}{\Delta x} \leq \frac{1}{\sqrt{2}} \tag{13}$$

As we will see in the following this condition poses some restrictions in the use of numerical schemes.

C. Absorbing Boundary Condition

In the acoustic tomography problem, ideally we do not have the boundary conditions and the medium is assumed to be infinitely large. But this assumption is not possible in numerical implementations, since the cost of the problem goes to infinity. For this purpose one can take the region of simulation larger than the real region of interest such that the effect of reflections from the boundaries do not appear at the time of receiving the desired signal in the receivers.

On the other hand it is possible to introduce artificial boundaries to limit the area of computation in a manner that they approximate the free space response. One needs boundary conditions at these artificial boundaries to guarantee a unique and well-posed solution to the wave equation [5].

To find the artificial boundaries that mimic the absorbing boundaries, according to [5] first assume that the conditions are applied to the left wall of the region at $x = 0$. The plane waves traveling to left can be formalized as

$$u(x, y, t) = e^{j(\frac{1}{c}k_x x + \frac{1}{c}k_y y + \omega t)} \tag{14}$$

Where $k_x = \sqrt{k_y^2 - \omega^2}$.

These waves satisfy the following condition for fixed (ω, k_y)

$$\Big(\frac{d}{dx} - \frac{j}{c}\sqrt{\omega^2 - k_y^2}\Big)u\Big|_{x=0} = 0. \tag{15}$$

This formulation means that if one has the above condition for the waves near the left wall, they are going only to the left direction and ideally no reflections happen. The same procedure can be done for wave packets of several frequencies and derive the relations, but the problem is such a condition for the boundary is non-local in space and time. So one needs to find boundary condition which is first local in space and time and second leads to well-posed mixed boundary value problem for the wave equation.

The trick is to simplify the expression in (15) with the approximation $\sqrt{1-k_y^2/\omega^2} = 1 - k_y^2/2\omega^2 + \mathcal{O}(k_y^4/\omega^4)$ made at $k_y = 0$ (perpendicular incidence angle). Thus the first approximation will be

$$\Big(\frac{d}{dx} - \frac{j\omega}{c}\Big)u\Big|_{x=0} = 0 \tag{16}$$

recalling that $j\omega$ corresponds to first derivative in time, one gets

1st approximation

$$\Big(\frac{\partial}{\partial x} - \frac{\partial}{c\partial t}\Big)u\Big|_{x=0} = 0. \tag{17}$$

2nd approximation

$$\Big(\frac{\partial^2}{\partial x \partial t} - \frac{\partial^2}{c\partial^2 t} + \frac{\partial^2}{2c\partial^2 y}\Big)u\Big|_{x=0} = 0. \tag{18}$$

It is shown in details in [5] that the above formulations of absorbing boundary conditions are both well-posed for wave equation.

Now for the numerical implementation of above formulas one can assume to have the grid (t^n, x_l,y_k), where:

$$\begin{cases} n = 0, 1, \ldots, n_{max} & t^n = n\Delta t \\ l = 0, 1, \ldots, l_{max} & x_l = l\Delta x \\ k = 0, 1, \ldots, k_{max} & y_k = k\Delta y \end{cases}$$

defining:

$$D_+(f) = \frac{f(x+h) - f(x)}{h}$$
$$D_-(f) = \frac{f(x) - f(x-h)}{h}$$
$$D_0(f) = \frac{f(x+h) - f(x-h)}{2h}$$

Equation (6) can be rewritten as

$$(D_+^t D_-^t - D_+^x D_-^x - D_+^y D_-^y)u_{l,k}^n = 0 \tag{19}$$

And for the absorbing boundary conditions

1st app.

$$D_+^x(u_{0,k}^n + u_{0,k}^{n+1}) - \frac{1}{c}D_+^t(u_{0,k}^n + u_{1,k}^n) = 0$$

Which leads to:

$$u_{0,k}^{n+1} = \frac{1}{c\Delta t + \Delta x}[u_{1,k}^{n+1}(c\Delta t - \Delta x) + u_{0,k}^n(\Delta x - c\Delta t) + u_{1,k}^n(\Delta x + c\Delta t)] \tag{20}$$

The second approximation can also be formalized as

2nd app.

$$D_0^t D_+^x u_{0,k}^n - \frac{1}{2c}D_+^t D_-^t(u_{0,k}^n + u_{1,k}^n) + \frac{c}{4}D_+^y D_-^y(u_{0,k}^{n-1} + u_{1,k}^{n+1}) \tag{21}$$

This leads to the relation:

$$\begin{aligned} u_{0,k}^{n+1} = {} & \frac{1}{(\frac{1}{2\Delta x\Delta t} + \frac{1}{2c\Delta t^2})} \times \\ & [u_{1,k}^{n+1}(\frac{1}{2\Delta x\Delta t} - \frac{1}{2c\Delta t^2} - \frac{c}{2\Delta x^2}) \\ & + u_{0,k}^{n-1}(\frac{1}{2\Delta x\Delta t} - \frac{1}{2c\Delta t^2} - \frac{c}{2\Delta y^2}) \\ & + u_{1,k}^{n-1}(\frac{-1}{2\Delta x\Delta t} - \frac{1}{2c\Delta t^2}) \\ & + u_{0,k}^{n}(\frac{1}{c\Delta t^2}) \\ & + u_{1,k}^{n}(\frac{1}{c\Delta t^2}) \\ & + \frac{c}{4\Delta y^2}(u_{0,k+1}^{n-1} + u_{1,k+1}^{n+1} + u_{0,k-1}^{n-1} + u_{1,k-1}^{n+1})] \end{aligned} \tag{22}$$

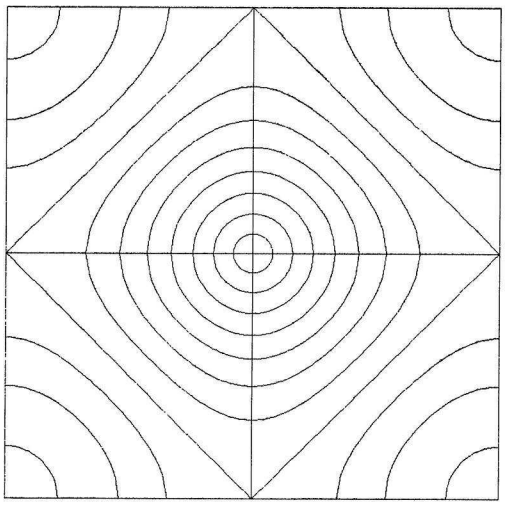

Fig. 2 – Dispersion plot of LF2, the horizontal axis is k_x and the vertical one is k_y. the lines are the fixed-ω curves starting from $\omega = \pi/8\Delta t$ to $\omega = 11\pi/8\Delta t$. the curves are getting more and more farther from a circle as the frequency goes larger. Image taken from [6].

For our case since the difference between the output of 1^{st} and 2^{nd} is not significant comparing the complexity, we preferred to use the 1^{st} approximation.

D. Numerical Dispersion Analysis

Assume that the following plane wave is the solution of a partial differential equation.

$$u(\mathbf{r}, t) = e^{j(\omega t - \mathbf{k}.\mathbf{r})} \tag{23}$$

and assume that for each real wave number vector $\mathbf{k}$, there exists a real frequency ω such that (23) is a solution. The relation

$$\omega = \omega(\mathbf{k}) \tag{24}$$

is called the *dispersion relation* for the corresponding differential equation [6].

The energy associated with wave number $\mathbf{k}$ moves asymptotically at the *group speed*

$$\mathbf{C}_g(\mathbf{k}) = \nabla_{\mathbf{k}}\omega \tag{25}$$

It is shown [6] that in the numerical implementation of the wave equation, the signals are moving with their group velocity rather than the phase velocity. Now let us consider the 2D wave equation (1) implemented by LF2 scheme as in (6). The dispersion relation for the analytical wave equation is

$$\omega^2 = k_x^2 + k_y^2 \tag{26}$$

But for LF2 this relation becomes [6]

$$\sin^2 \frac{\omega\Delta t}{2} = \lambda^2[\sin^2 \frac{k_x\Delta x}{2} + \sin^2 \frac{k_y\Delta x}{2}]. \tag{27}$$

This relation is plotted in Fig.2. In [6], it is assumed that a plane wave is traveling with θ as the angle from the x axis of the normal to it. Then the group speed and traveling angle become

$$|\mathbf{C}_g| = \frac{\lambda\sqrt{\sin^2 k_x\Delta x + \sin^2 k_y\Delta x}}{\sin\omega\Delta t}, \tag{28}$$

$$\Theta = \tan^{-1}\left(\frac{\sin k_y\Delta y}{\sin k_x\Delta x}\right). \tag{29}$$

The above expressions to the second order are

$$|\mathbf{C}_g| \approx c - \frac{(|\mathbf{k}|\Delta x)^2}{8}[\frac{3+\cos 4\theta}{4} - \lambda^2], \tag{30}$$

$$\Theta \approx \theta + \frac{(|\mathbf{k}|\Delta x)^2}{24}\sin 4\theta. \tag{31}$$

These equations show that with small choice of $|\mathbf{k}|\Delta x$, the numerical dispersion can be canceled.

E. Limitations

As illustrated before, one can easily see that numerical dispersion is a non-separable fact from numerical implementations In LF2 as will be depicted in next chapter (Fig.7), this effect causes very bad artifacts which make the simulation inaccurate for our application. The goal is to overcome this effect. One natural idea can be to make the space grid size (Δx) smaller. But as illustrated in the beginning of the chapter this means that more number of samples should be collected and larger matrices must be used in the simulations, therefor the computation and memory cost grows exponentially with this factor.

Even if one overcomes this problem with simulations, the C.F.L. condition implies that the space steps can't be arbitrarily small while the time steps are kept fix. The ratio between them must be constant and less than $1/\sqrt{2}$. Which means that one would also need to decrease Δt as well, and this would imply iterations and complexity in the algorithm.

F. ONADM Scheme

This recently proposed method by Yang et al. as indicated in [7] is called Optimal Nearly Analytic Discrete Method (ONADM). For computational purposes they define

$$\mathbf{u}_{i,j}^n = \begin{pmatrix} u \\ \frac{\partial u}{\partial x} \\ \frac{\partial u}{\partial y} \end{pmatrix}_{i,j}^n$$

Obviously all of components of this matrix satisfy the wave equation provided that u satisfies it. If one writes the Taylor series expansion of $\mathbf{u}_{i,j}^{n+1}$ and $\mathbf{u}_{i,j}^{n-1}$ as

$$\begin{aligned}\mathbf{u}_{i,j}^{n+1} = \mathbf{u}_{i,j}^n &+ \Delta t(\frac{\partial \mathbf{u}}{\partial t})_{i,j}^n + \frac{\Delta t^2}{2}(\frac{\partial^2 \mathbf{u}}{\partial t^2})_{i,j}^n \\ &+ \frac{\Delta t^3}{6}(\frac{\partial^3 \mathbf{u}}{\partial t^3})_{i,j}^n + \frac{\Delta t^4}{24}(\frac{\partial^4 \mathbf{u}}{\partial t^4})_{i,j}^n,\end{aligned} \tag{32}$$

$$\begin{aligned}\mathbf{u}_{i,j}^{n-1} = \mathbf{u}_{i,j}^n &- \Delta t(\frac{\partial \mathbf{u}}{\partial t})_{i,j}^n + \frac{\Delta t^2}{2}(\frac{\partial^2 \mathbf{u}}{\partial t^2})_{i,j}^n \\ &- \frac{\Delta t^3}{6}(\frac{\partial^3 \mathbf{u}}{\partial t^3})_{i,j}^n + \frac{\Delta t^4}{24}(\frac{\partial^4 \mathbf{u}}{\partial t^4})_{i,j}^n.\end{aligned} \tag{33}$$

Adding (32) and (33) together one gets

$$\mathbf{u}_{i,j}^{n+1} = 2\mathbf{u}_{i,j}^n - \mathbf{u}_{i,j}^{n-1} + \Delta t^2\Big(\frac{\partial^2 \mathbf{u}}{\partial t^2}\Big)_{i,j}^n + \frac{\Delta t^4}{12}\Big(\frac{\partial^4 \mathbf{u}}{\partial t^4}\Big)_{i,j}^n. \tag{34}$$

After substituting the appropriate values for $\left(\frac{\partial^2 \mathbf{u}}{\partial t^2}\right)_{i,j}^n$ and $\left(\frac{\partial^4 \mathbf{u}}{\partial t^4}\right)_{i,j}^n$ according to wave equation, the result will be

$$\begin{aligned}\mathbf{u}_{i,j}^{n+1} =& 2\mathbf{u}_{i,j}^n - \mathbf{u}_{i,j}^{n-1} \\ &+ (c_{i,j}\Delta t)^2[(\frac{\partial^2 \mathbf{u}}{\partial x^2})_{i,j}^n + (\frac{\partial^2 \mathbf{u}}{\partial y^2})_{i,j}^n] \\ &+ \frac{(c_{i,j}\Delta t)^4}{12}[(\frac{\partial^4 \mathbf{u}}{\partial x^4})_{i,j}^n + 2(\frac{\partial^4 \mathbf{u}}{\partial x^2 \partial y^2})_{i,j}^n + (\frac{\partial^4 \mathbf{u}}{\partial y^4})_{i,j}^n].\end{aligned} \tag{35}$$

The values of the derivatives are derived in [7] and the key difference of this method with other ones is that first it uses also first derivative of u in space for updating the values in time, which causes one more order of approximation accuracy, and second the way these derivatives are updates, which incorporates the previous values of u, $\partial u/\partial x$ and $\partial u/\partial y$.

For computing the higher order derivatives of u, according to [8] they define an interpolation function

$$G(\Delta x, \Delta y) = \sum_{r=0}^{5} \frac{1}{r!}(\Delta x\frac{\partial}{\partial x} + \Delta y\frac{\partial}{\partial y})^r u, \tag{36}$$

and higher order derivative of u are defined in relation to higher order derivatives of $G(\Delta x, \Delta y)$ with respect to Δx and Δy. So if one imagines that the values for $u_{i,j}^n$, $(\partial u/\partial x)_{i,j}^n$ and $(\partial u/\partial y)_{i,j}^n$are stored in $\mathbf{U}^n$, $\mathbf{V}^n$ and $\mathbf{H}^n$ respectively, would have

$$\begin{aligned}\mathbf{U}^{n+1} &= 2\mathbf{U}^{n} - \mathbf{U}^{n-1} \\ &+ \frac{\Delta t^2}{\Delta x^2}\mathbf{C}^{②} \odot \Big[(\mathbf{U}^{n} * \mathbf{A}_{u1}) + \frac{\Delta t^2}{\Delta x^2}\mathbf{C}^{②} \odot (\mathbf{U}^{n} * \mathbf{A}_{u2})\Big] \\ &+ \frac{\Delta t^2}{\Delta x}\mathbf{C}^{②} \odot \Big[(\mathbf{V}^{n} * \mathbf{B}_{u1}) + \frac{\Delta t^2}{\Delta x^2}\mathbf{C}^{②} \odot (\mathbf{V}^{n} * \mathbf{B}_{u2})\Big] \\ &+ \frac{\Delta t^2}{\Delta x}\mathbf{C}^{②} \odot \Big[(\mathbf{H}^{n} * \mathbf{D}_{u1}) + \frac{\Delta t^2}{\Delta x^2}\mathbf{C}^{②} \odot (\mathbf{H}^{n} * \mathbf{D}_{u2})\Big],\end{aligned} \tag{37}$$

where we have

$$\mathbf{A}_{u1} = \begin{bmatrix} 0 & 2 & 0 \\ 2 & -8 & 2 \\ 0 & 2 & 0 \end{bmatrix}, \qquad \mathbf{A}_{u2} = \begin{bmatrix} 1/6 & -4/3 & 1/6 \\ -4/3 & 14/3 & -4/3 \\ 1/6 & -4/3 & 1/6 \end{bmatrix}$$

$$\mathbf{B}_{u1} = \begin{bmatrix} 0 & 0 & 0 \\ -1/2 & 0 & 1/2 \\ 0 & 0 & 0 \end{bmatrix}, \qquad \mathbf{B}_{u2} = \begin{bmatrix} 0 & 0 & 0 \\ 1/2 & 0 & -1/2 \\ 0 & 0 & 0 \end{bmatrix}$$

$$\mathbf{D}_{u1} = \mathbf{B}_{u1}^{T}, \qquad \mathbf{D}_{u2} = \mathbf{B}_{u2}^{T}.$$

The procedure for updating the derivative matrices, $\mathbf{V}$ and $\mathbf{H}$ is the same and but with different filters and coefficients.

1) Stability Criteria: As indicated in [7], the stability condition in this method requires that

$$\lambda = \frac{c_{\max}\Delta t}{\Delta x} \leq 0.527. \tag{38}$$

Which is less than what we have seen for LF2 scheme and the simulation parameters are more restricted, but as the order of approximation is more here and also the use of higher derivatives, it is expected to get better results which is confirmed by the simulations.

G. Implicit Methods

For these schemes we will just give an small example and will justify the impossibility of their usage in our case. For simplicity consider a 1D wave equation

$$\frac{\partial^2 u}{\partial t^2} = c^2 \frac{\partial^2 u}{\partial x^2}. \tag{39}$$

One of the implicit methods used is the backward difference method. According to this scheme we approximate the wave equation as

$$\frac{u_j^{n+1} - 2u_j^{n} + u_j^{n-1}}{c^2\Delta t^2} = \frac{u_{j+1}^{n+1} - 2u_j^{n+1} + u_{j-1}^{n+1}}{\Delta x^2}, \tag{40}$$

which can be rearranged as

$$(1+2\lambda^2)u_j^{n+1} - \lambda^2(u_{j+1}^{n+1} + u_{j-1}^{n+1}) = 2u_j^{n} - u_j^{n-1}. \tag{41}$$

Following one can write this as a system of $M-1$ equations with $M-1$ unknowns, where $j = 0, 1, \cdots, M$. In the matrix format

$$\begin{bmatrix} 1+2\lambda^2 & -\lambda^2 & & & \\ -\lambda^2 & 1+2\lambda^2 & -\lambda^2 & & \\ & \ddots & \ddots & \ddots & \\ & & -\lambda^2 & 1+2\lambda^2 & -\lambda^2 \\ & & & -\lambda^2 & 1+2\lambda^2 \end{bmatrix} \begin{bmatrix} u_1^{n+1} \\ u_2^{n+1} \\ \vdots \\ u_{M-1}^{n+1} \end{bmatrix} = \begin{bmatrix} 2u_1^{n} - u_1^{n-1} \\ 2u_2^{n} - u_2^{n-1} \\ \vdots \\ 2u_{M-1}^{n} - u_{M-1}^{n-1} \end{bmatrix}. \tag{42}$$

Thus solving this set of equations is equal to finding the current values of the sound pressure from previous time samples.

The biggest advantage of implicit methods is that they don't have the stability condition and they are unconditionally stable. But the limitation for these schemes comes immediately by looking to the updating matrix. The boundary values are not updated in this process and assumed to be zero so these methods are only usable for initial boundary value problems, where the boundary values for different times are known and fixed. Since the nature of problem is not boundary value problem, we are unable to use these algorithms in finding wave equation results.

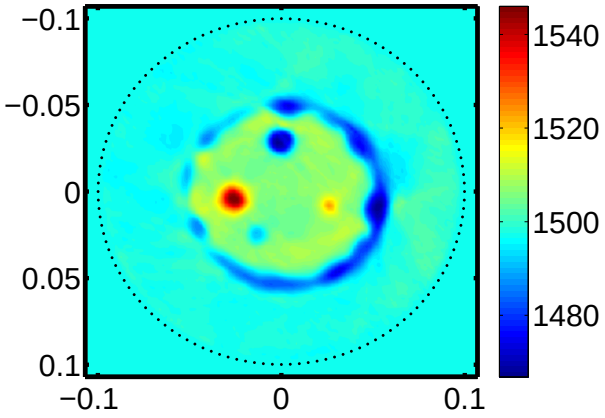

Fig. 3 – The measurement setup for acoustic tomography of breast. Sensors are deployed on a $20\ cm$ diameter circle. For the simulations we used a phantom that is illustrated in figure.

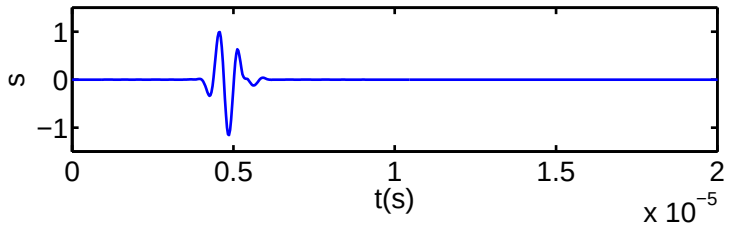

Fig. 4 – The source signal used in the simulations.

III. Simulations and Discussions

For the simulations two possible media are assumed. One is the homogeneous medium with sound speed on $1497\ m/s$ and the other one the same medium but containing a breast phantom. It is assumed that there are 256 sensors deployed around the phantom on a circle with diameter $20\ cm$. The temporal step size is taken to be $\Delta t = 3.2 \times 10^{-8}\ s$ and the spatial step size is $\Delta x = 1 \times 10^{-4}\ m$. So that the ratio $\lambda = c\Delta t/\Delta x = 0.479$ is satisfying the stability condition for both LF2 and ONADM schemes. The shape of the phantom and the sensors is depicted in Fig.3. The sent signal is chosen to be a smooth version of what is sent in real measurements and is depicted in Fig.4.

A. LF2 Scheme

As discussed in the previous chapter, the LF2 scheme can be written in matrix format as

$$\mathbf{U}^{n+1} = 2\mathbf{U}^{n} - \mathbf{U}^{n-1} + \frac{\Delta t^2}{\Delta x^2}\mathbf{C}^{②} \odot (\mathbf{U}^{n} * \mathbf{h}) \tag{43}$$

The sent signal is the same as illustrated in Fig.4. The output without assumption of absorbing boundary condition is illustrated in Fig.5. As can be seen in the figure, the waves are gotten fatter and high frequency parts of the signal are behind and traveling with lower speed.

B. Absorbing Boundary Condition

For this part the absorbing boundary condition is imposed to all 4 walls of the region of interest. The first approximation is used for the walls and the results are depicted in Fig.6. The maximum peak of the reflected waves are less than 5% of the incident waves in the reflection point. It is also worth mentioning that since the approximation was done in $k_y = 0$, namely perpendicular to the walls, the waves hitting the wall with larger angles get more reflected and most of the reflectances are due to these angles.

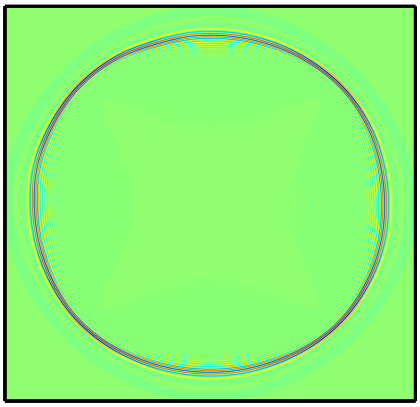

Fig. 5 – The waves propagating as the result of LF2 scheme.

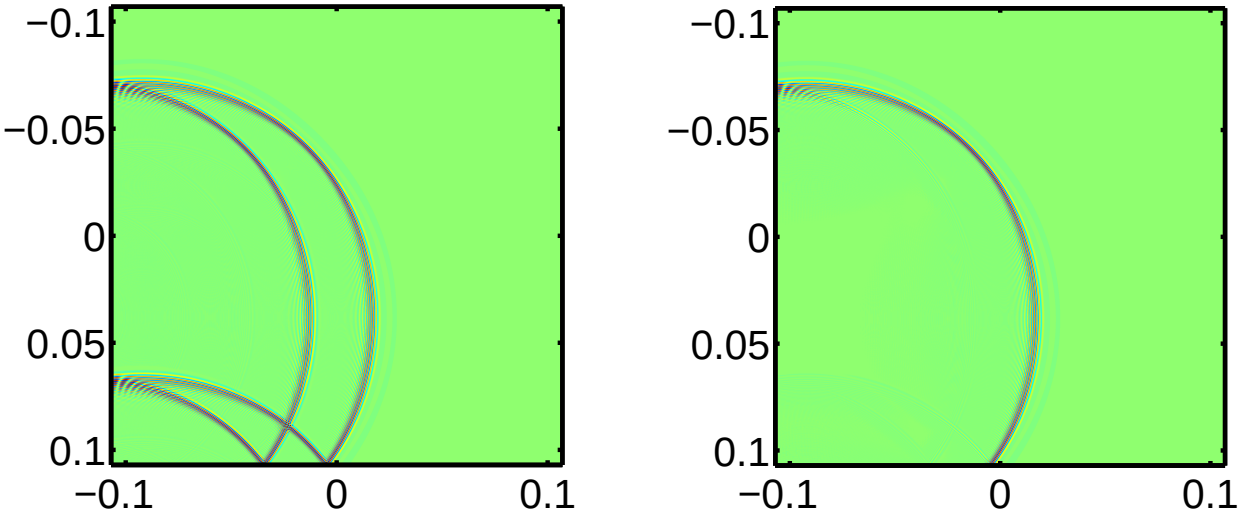

(a) (b)

Fig. 6 – (a) field values as the result of LF2 scheme without implementation of absorbing boundary condition, (b)Field values after implementation of absorbing boundary conditions. It is seen that most part of the reflectances occur due to the direct signal from source and in large degree angles.

C. ONADM Scheme

For this purpose the ONADM scheme was implemented and the results comparing to those of LF2 is shown in Fig.7. as can be seen from the figure, there is no more numerical dispersion visible and the shape of propagation is preserved as expected. This implies that although the stability of ONADM is more restricted than LF2, the results for higher step sizes compensate this problem and the choice of smaller step sizes is not considered any more. Another experiment is also depicted in Fig.8. In this figure we are considering two cases, in the above figure, the two signals correspond to the signals received in receiver for homogeneous and inhomogeneous cases respectively, where the transmitter is sensor number 1 and the receiver is sensor number 150. In the below figure, the two signals are the simulated corresponds of the above ones. Please pay attention to the rightmost part of the signals below which shows the effect of reflectance which comes behind the signal.

REFERENCES

[1] I. Jovanovic, *Inverse problems in acoustic tomography*, PhD thesis, Lausanne, 2008.
[2] M. A. Jensen, *Computational Electromagnetics Course Notes*, 2005.
[3] A. R. Mitchel, *Computational Methods in Partial Differential Equations*, John Wiley & Sons, 1969.

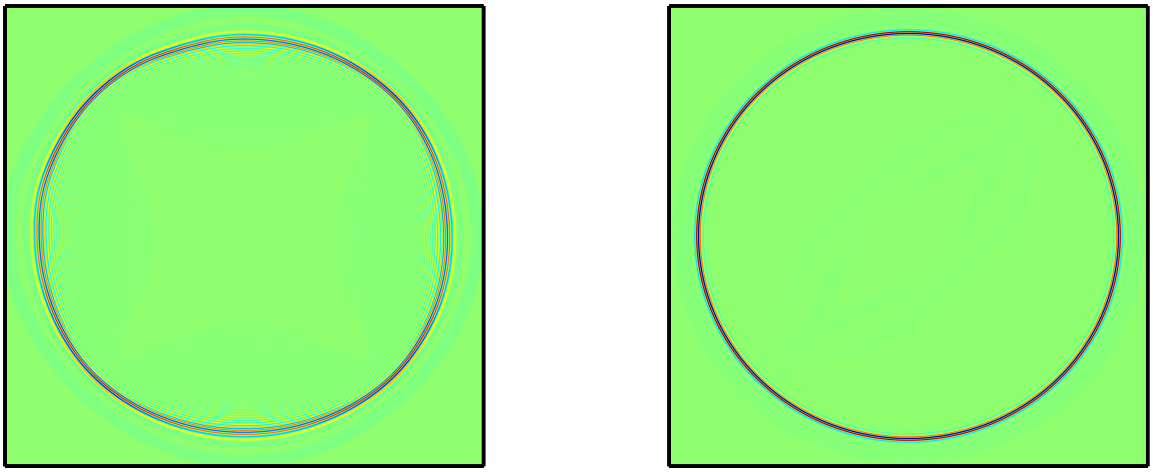

(a) (b)

Fig. 7 – (a) field values as the result of LF2 scheme, (b)Field values as the result of ONADM scheme. The numerical dispersion effects is not visible anymore in (b) and the circle shape of traveling is preserved.

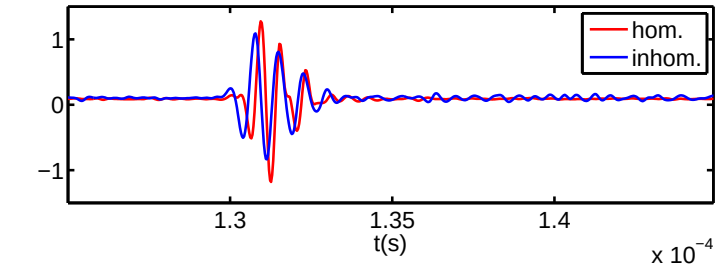

(a)

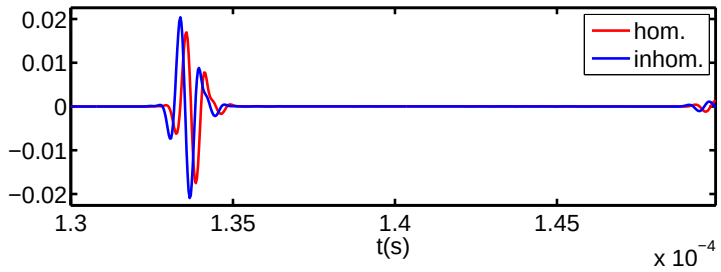

(b)

Fig. 8 – (a) Received signals in homogeneous medium and inhomogeneous case in the real setup of experiment, (b) Received signals in homogeneous medium and inhomogeneous case in the simulations.

[4] R. Courant, K. Friedrichs, and H. Lewy, Über die partiellen Differenzengleichungen der mathematischen Physik, Mathematische Annalen **100**(1), 32–74 (1928).
[5] B. Engquist and A. Majda, Absorbing Boundary Conditions for the Numerical Simulation of Waves, Mathematics of Computation **31**(139), 629–651 (1977).
[6] L. N. Trefethen, Group Velocity in Finite Difference Schemes, Technical report, Stanford, CA, USA, 1981.
[7] D. Yang, J. Peng, M. Lu, and T. Terlaky, Optimal Nearly analyticc Discrete Approximation ot the Scalar Wave Equation, Bulletin of the Seismological Society of America **96**(3), 1114–1130 (2006).
[8] Y. Konddoh, Y. Hosaka, and K. Ishii, Kernel Optimum Nearly analytical Discretization Algorithm Applied to Parabolic and Hyperbolic Equations, Comp. Math. Appl. **27**, 59–90 (1994).